Available online at www.sciencedirect.com

SCIENCE DIRECT®

Earth and Planetary Science Letters 224 (2004) 131–141

EPSL

www.elsevier.com/locate/epsl

Trace-element evidence for the origin of desert varnish by direct aqueous atmospheric deposition

Nivedita Thiagarajan, Cin-Ty Aeolus Lee*

Department of Earth Science, MS-126, Rice University, Houston, TX 77005, USA

Received 7 November 2003; received in revised form 26 April 2004; accepted 29 April 2004

Abstract

Smooth rock surfaces in arid environments are often covered with a thin coating of Fe–Mn oxyhydroxides known as desert varnish. It is debated whether such varnish is formed (a) by slow diagenesis of dust particles deposited on rock surfaces, (b) by leaching from the underlying rock substrate, or (c) by direct deposition of dissolved constituents in the atmosphere. Varnishes collected from smooth rock surfaces in the Mojave Desert and Death Valley, California are shown here to have highly enriched and fractionated trace-element abundances relative to upper continental crust (UCC). They are highly enriched in Co, Ni, Pb and the rare-earth elements (REEs). In particular, they have anomalously high Ce/La and low Y/Ho ratios. These features can only be explained by preferential scavenging of Co, Ni, Pb and the REEs by Fe–Mn oxyhydroxides in an aqueous environment. High field strength elements (HFSEs: Zr, Hf, Ta, Nb, Th), however, show only small enrichments despite the fact that these elements should also be strongly scavenged by Fe–Mn oxyhydroxides. This suggests that their lack of enrichment is a feature inherited from a solution initially poor in HFSEs.

The first two scenarios for varnish formation can be ruled out as follows. The high enrichment factors of Fe, Mn and many trace elements cannot be generated by mass loss associated with post-depositional diagenesis of dust particles because such a process predicts only a small increase in concentration. In addition, the highly fractionated abundance patterns of particle reactive element pairs (e.g., Ce/La and Y/Ho) rules out leaching of the rock substrate. This is because if leaching were to occur, varnishes would grow from the inside to the outside, and thus any particle-reactive trace element leached from the substrate would be quantitatively sequestered in the Fe–Mn oxyhydroxide layers, prohibiting any significant elemental fractionations. One remaining possibility is that the Fe, Mn and trace metals in varnish are derived from leaching of dust particles entrained in rain or fog droplets either in the atmosphere or during wet atmospheric deposition. The high trace metal enrichment factors require that most of the dust was physically removed before or during varnish formation. The remaining aqueous counterpart would be depleted in HFSEs and Th relative to the REEs, Co, Ni and Pb because the former are more insoluble and hence largely retained in the removed dust fraction. The high Ce/La ratios suggest that precipitation of trace metals may have been governed by equilibrium partitioning in an excess of wet atmospheric deposition. If varnishes are indeed derived from wet atmospheric deposition, they may provide a record of the aqueous component of atmospheric dust inputs to various environments.

Keywords: varnish; iron; manganese; trace element; aqueous

* Corresponding author. Tel.: +1-713-348-5084; fax: +1-713-348-5214.
E-mail address: ctlee@rice.edu (C.-T. Aeolus Lee).

0012-821X/$ - see front matter © 2004 Elsevier B.V. All rights reserved.
doi:10.1016/j.epsl.2004.04.038

1. Introduction

Rock surfaces in arid environments are often thinly (<200 μm) coated with a dark and shiny substance called desert varnish [1]. Such coatings represent a fine mixture of clay minerals and Fe–Mn oxyhydroxides, which form micrometer-thick laminations that parallel the topography of the rock substrate [2]. There is still considerable debate over how varnish forms. The debate can be simplified to three end-member scenarios [1,3]:

Model 1: direct leaching of the rock substrate followed by re-precipitation on the rock surface;
Model 2: slow (1000+ years) diagenesis of detrital dust particles *after* accretion to the rock substrate; and
Model 3: direct chemical precipitation of dissolved atmospheric components in rain water, fog droplets or aerosols (both of these processes can be microbially mediated [4,5]).

Several lines of argument have been used to suggest that varnishes are probably extraneous to the rock substrate on which they are deposited (see Dorn [4] for a review on other types of Fe–Mn surface coatings that are derived from the host rock) and that they have an atmospheric origin: The contact between the varnish and the rock substrate is texturally abrupt; varnishes occur on nearly all rock types, including quartzites, which have little or no Fe, Mn and clay minerals [2]; they contain a high diversity of clay minerals that could not have all been generated in situ [2]; they contain small amounts of sulfate whose oxygen isotopic signature is uniquely atmospheric [6]; and they contain measurable quantities of ^{210}Pb, a short-lived natural radionuclide that exists in the atmosphere due to the decay of ^{222}Rn that leaks from soils [7]. The possibility of an atmospheric origin has led many to explore whether the chemical make-up of varnish can be used to extract paleo-climatic information in the Quaternary [1,8]. It has also been recognized that varnishes harbor microbial communities that may mediate the formation of Fe and Mn oxyhydroxides [3,5,9]. Finally, the ubiquity of varnish in arid environments has led to speculation that varnishes may have Martian analogs [10,11].

In order to provide an independent means of differentiating these three hypotheses, we investigate here the trace metal systematics of a small collection of desert varnishes from southwestern USA. In particular, we focus on those elements that are known to be preferentially scavenged by Fe and Mn oxyhydroxides in aqueous environments. Each of the above scenarios predicts different levels of trace metal enrichments and fractionations.

2. Samples and methods

Varnishes were collected from surfaces of Pliocene and younger basaltic lavas in southeastern California (coordinates given in Table 1). Three varnishes (OF14.5, MC14, MC36) are from the tops of dated lava flows in the Cima volcanic field in the Mojave Desert [12]. These flows form topographical highs and preserve the original morphology of the flow surface. The effects of overland water flow are hence minimal. The fourth varnish sample is from "desert pavement" in Death Valley (BM), a geomorphic surface made up of varnished rock clasts resting on top of a fine matrix of wind-blown sediment [13]. We also analyzed two sections of a marine Fe–Mn crust from a South Pacific seamount; Fe–Mn crusts are formed by direct chemical precipitation from seawater and were investigated because their mode of formation may shed light on the aqueous atmospheric deposition hypothesis for varnish formation described above [14].

Since varnishes are very thin, it is nearly impossible to flake off a piece of varnish to study. Instead, we used a high-purity quartz rod to very gently scrape the surface of the varnishes in a clean laboratory environment, generating fine-grained varnish powders. Parrafin wax was used to cover the parts of the rock from which we did not want to sample. Before scraping, the exposed varnish surface was gently cleaned with a clean tissue lightly soaked with alcohol. We specifically sampled very smooth varnish surfaces because it was easier to scrape off pure varnish on smooth surfaces than on rough surfaces. Because of the thinness of the varnish, a very large surface area (>100 cm^2) was scraped in order to obtain enough powder to measure. Care was taken to avoid scraping through the varnish and into the underlying

Table 1

	Varnish (Death Valley)		Varnish (Mojave Desert)					South Pacific Fe–Mn Crust	
	Bm		OF14.5		MC14		MC36	Mi3	Mi17
Latitude (°)	36.34		35.18		35.20		35.26		
Longitude (°)	117.18		115.77		115.87		115.72		
Basalt age (Myears)			0.35		0.16		0.33		
	a	b	a	b	a	b			
	ppm	ppm	ppm	ppm	ppm	ppm	ppm	ppm	ppm
Li	173	202	60.8	54.0	102	99.6	65.7	1.39	1.19
Be	4.40	4.34	2.55	2.94	5.45	5.00	2.90	4.84	4.02
Sc	35.9	44.7	22.7	28.4	33.4	36.6	31.0	7.95	6.82
V	332	365	236	254	302	330	314	674	466
Cr	210	213	259	387	547	324	1822	795	299
Co	179	175	115	128	226	232	217	7200	2500
Ni	128	106	203	170	246	247	381	4218	3937
Cu	118	81.0	n/a	105	131	109	112	471	774
Zn	269	201	229	234	264	280	345	615	504
Ga	33.3	28.7	28.5	29.4	n/a	42.3	31.7	42.3	29.3
Rb	30.5	20.7	51.7	53.5	44.7	45.1	28.8	3.59	1.97
Sr	551	597	470	469	377	406	350	1489	1318
Y	61.4	41.3	35.6	35.9	85.9	87.9	45.1	202	187
Zr	304	318	277	273	278	307	281	588	485
Nb	19.2	21.2	45.5	46.4	43.9	49.5	54.0	52.1	27.1
Mo	5.91	6.27	12.0	14.7	9.67	10.1	10.4	592	573
Cd	8.26	8.69	3.27	3.31	11.4	12.1	6.25	5.10	4.19
Sn	6.23	5.74	3.63	4.20	4.20	4.36	4.83	10.6	11.9
Te	0.631	0.670	0.221	0.370	0.538	0.535	0.490	43.2	33.1
Cs	1.74	1.35	1.83	2.34	3.18	3.30	1.53	0.075	0.056
Ba	1417	1409	1802	1881	1641	1834	1479	1486	1407
La	113	43.1	69.4	60.5	173.0	194.2	63.0	176	131
Ce	533	393	351	415	1391	1628	428	609	775
Pr	24.0	13.0	14.7	14.9	39.3	40.3	15.6	26.1	20.1
Nd	86.8	51.7	57.6	59.6	135.1	149	70.3	120	88.9
Sm	18.0	12.3	11.6	12.3	28.6	29.9	15.3	26.0	18.4
Eu	4.52	3.32	3.66	3.89	6.84	6.82	3.51	6.64	4.77
Tb	2.95	2.04	1.83	1.95	4.51	4.54	2.02	5.21	3.34
Gd	18.7	12.3	11.9	12.3	28.4	29.6	13.8	36.0	21.7
Dy	15.7	11.5	9.45	10.4	23.5	23.9	11.7	35.8	21.3
Ho	2.82	2.16	1.63	1.84	4.15	4.49	1.89	7.44	3.25
Er	7.87	6.14	4.36	5.06	11.4	12.57	5.43	24.6	13.9
Tm	1.12	0.847	0.606	0.685	1.627	1.706	0.701	3.563	2.076
Yb	7.38	5.50	3.97	4.49	10.6	11.0	5.36	25.7	14.9
Lu	1.10	0.817	0.580	0.650	1.56	1.64	0.621	3.71	2.15
Hf	7.89	8.02	7.14	7.33	7.90	8.51	7.56	10.6	6.78
Ta	0.895	1.08	2.21	2.61	2.57	2.99	2.88	1.10	0.469
W	77.6	75.2	11.6	18.2	10.5	11.1	14.8	109	80.9
Tl	3.53	3.45	1.49	1.30	5.68	6.27	0.71	153	112
Pb	614	584	105	192	258	275	261	1257	607
Bi	2.80	2.78	0.64	1.21	1.31	1.35	1.67	28.69	34.28
Th	26.2	35.9	18.8	22.2	42.2	43.7	21.03	4.46	1.92
U	14.3	17.4	9.56	14.7	11.7	13.1	12.0	13.9	7.20
Mn	20,349	20,582	11,801	14,466	35,767	29,695	13,769	179,168	n/a
Fe	87,347	84,732	81,272	77,006	112,928	93,679	126,619	112,469	n/a

rock substrate. A total of 10–15 mg of varnish powder was obtained from each rock sample. We did not subsequently homogenize these powders for fear of contaminating such small sample quantities. For each analysis, 4–8 mg of varnish was dissolved. An ion blower was used to reduce static in the weighing room, allowing sample aliquots to be weighed to a precision of 2% relative standard deviation. Samples were dissolved using a 1:2 mixture of HF:HNO_3 and heated overnight at 120 °C. This was followed by drying down the sample and redissolving the precipitate in 2% HNO_3 with a trace of HCl and HF.

The final solution was analyzed for trace-element abundances using the Rice University Finnigan Element 2 inductively coupled plasma mass spectrometer (magnetic and electrostatic mass analyzers). Mass scans were performed using a combination of magnet jumps and scans with the electrostatic analyzer. Trace elements were analyzed at low resolution mode ($m/\Delta m \sim 300$) in which instrument sensitivity is maximized. Eu data were not reported due to $Ba^{16}O^{+}$ interferences. Although our BaO^{+}/Ba^{+} production is typically less than 1%, Ba concentrations were ~3 orders of magnitude higher than Eu concentrations, making it impossible to make proper interference corrections. Fe, Mn, V and Sc were analyzed at medium resolution ($m/\Delta m \sim 3000$) in order to differentiate their mass peaks from isobaric molecular ion interferences. Magnetic drifts were corrected by locking the mass calibration to $^{40}Ar^{16}O^{+}$. Hysteresis offsets were systematic and therefore could be corrected for by applying constant mass offsets to scans.

For all elements, except for Zr, Hf, Nb and Ta, concentrations were determined using fresh synthetic multi-element standards and an internal standard (In) to correct for drift. Zr and Hf were determined by mixing known quantities of ^{94}Zr and ^{180}Hf isotope tracers with the sample. Nb and Ta concentrations were determined by measuring the $^{93}Nb/^{90}Zr$, $^{93}Nb/^{91}Zr$, $^{93}Nb/^{92}Zr$, $^{181}Ta/^{177}Hf$, $^{181}Ta/^{178}Hf$ and $^{181}Ta/^{179}Hf$ ratios and normalizing to the Zr and Hf concentrations determined by isotope dilution. Because the enriched Zr and Hf isotope tracers are nearly pure, all three Nb/Zr and Ta/Hf ratios gave identical results to within error (<1%). Two international rock standards (United States Geological Survey BHVO-1 and BHVO-2) were used for quality control. Abundances are reported for elements for which the procedural blanks are less than 5% of the concentrations in the samples and rock standards.

3. Results

3.1. Varnishes

The varnish samples were found to have a Fe+Mn content of 8–15 wt.%. If the Fe and Mn are present as oxides or oxyhydroxides (Fe_2O_3, $Fe(OH)_3$, MnO_2, $Mn(OH)_4$), roughly 25–30% of these varnishes are made of Fe–Mn oxyhydroxides. This is consistent with previous observations that clays make up the remaining ~70% [2]. Mn content ranges from 1 to 4 wt.%, which is ~2 orders of magnitude higher than that in upper continental crust (UCC [15]). Many trace elements also appear to be highly enriched relative to UCC. Fig. 1 shows selected elemental abundances normalized to estimates of the average composition of UCC. For readability, UCC-normalized abundances are plotted in approximate order of increasing enrichment relative to UCC in Fig. 1A. Th and U are plotted next to each other to emphasize their similar behaviors in magmatic processes and contrasting behaviors in aqueous processes. Also plotted is the average normalized REE concentration *excluding* Ce, which we plot separately in Fig. 1B.

The alkali Earth metals show variable enrichments and depletions. Rb and Cs are extremely depleted relative to UCC, but Li, Be and Ba are highly enriched and Sr shows no significant enrichment or depletion. With the exception of Li, Zn, Cu, Ba and U, most trace-element enrichments are correlated with Mn concentration (Fig. 3). Co, Cr, Pb and Ni have the highest enrichments, ranging from 5 to 50 times that of UCC. Zn, Cu, V, Sc, Y and the rare-earth elements (REEs) are also enriched, but only by 2–10 times that of UCC. The rare-earth element Ce is enriched by ~4 times greater than neighboring REEs (Figs. 1B and 2A), resulting in strong positive Ce anomalies, which are typically not seen in magmatic processes. The elemental pair Y/Ho is also very difficult to fractionate during most magmatic processes, but the average Y/Ho of the varnishes are 20.4±1.7, which differs from typical magmatic values of 28. We further find

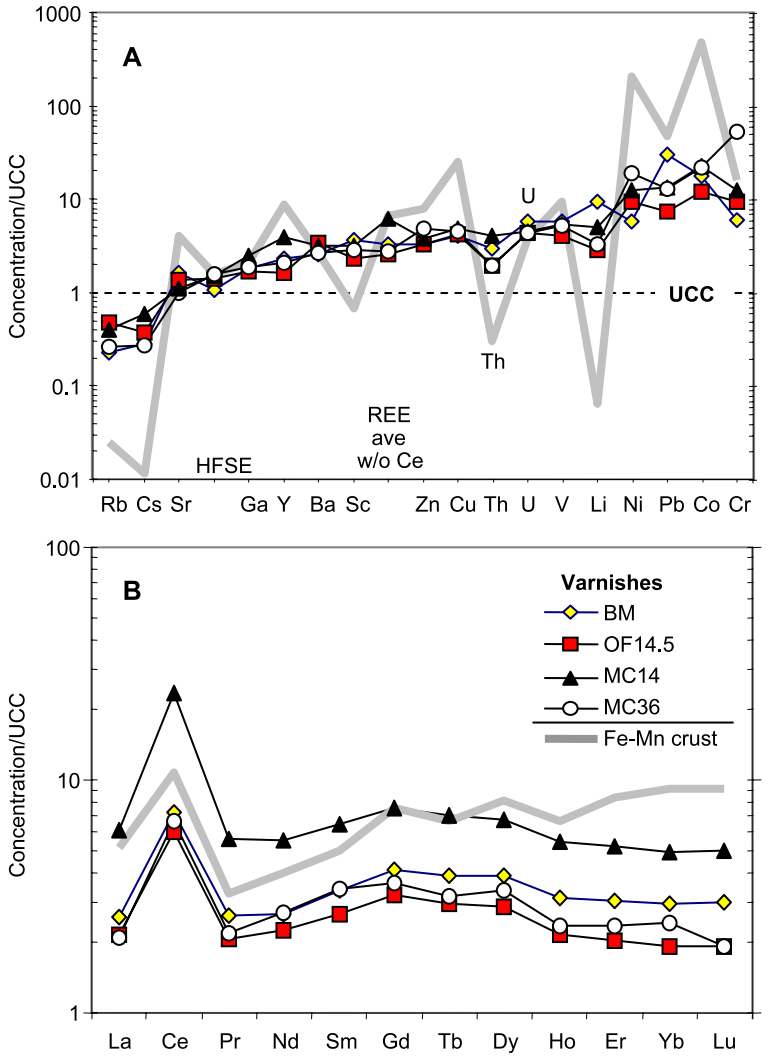

Fig. 1. Abundances of trace elements in varnish coatings normalized to average upper continental crust (UCC; [15]). For readability, elements in (A) are ordered in approximate order of increasing abundance with the exception of Th, which is placed by U to emphasize their similar behaviors in magmatic processes but contrasting solubilities in aqueous processes. Average normalized rare-earth element concentrations (REE ave) in (A) *do not include* Ce. UCC-normalized rare-earth element concentrations shown in (B). Thick gray line in (A) and (B) represents the average of two Fe–Mn crusts from the South Pacific.

that although Th and U are enriched by two to seven times, the relative enrichment of Th is less pronounced than that of U, resulting in a depleted Th/U ratio for some samples (Fig. 1A). The high field strength elements (HFSEs), Zr, Nb, Hf, and Ta, show only small (<2 times) enrichments (Fig. 1A). The average Zr/Hf ratio of the varnishes, 39.2±2 (1 S.D.), is higher than the value for UCC (32.8 [15]) but slightly lower than the value for Cima basalts (43.5±3 [16]).

3.2. Fe–Mn crusts

The trace-element abundance patterns of the Fe–Mn crusts are roughly similar to those of the varnishes (Fig. 1). For example, the Fe–Mn crusts are enriched

in the REEs, Ni, Pb and Co, have positive Ce anomalies, and are highly depleted in Rb and Cs. However, the Fe–Mn crusts differ from the varnishes in detail. Although the Fe–Mn crusts have positive Ce anomalies, they are slightly depleted in the light REEs relative to the heavy REEs in contrast to the somewhat flatter pattern seen in varnishes (Fig. 1B). In addition, the depletions in Rb, Cs and Th are much more extreme in Fe–Mn crusts, and Li also appears to be depleted in Fe–Mn crusts relative to the varnishes. Finally, the Fe–Mn crusts appear to be relatively more enriched in Co.

4. Discussion

4.1. An aqueous origin for trace elements in varnish

The trace-element abundance patterns described above require an aqueous origin because the relative enrichments or depletions of each element appear to qualitatively reflect their relative solubilities and/or their propensity for being scavenged by Fe–Mn oxyhydroxides. We highlight below the most significants trace element signatures.

Depletions in Rb and Cs: The extreme depletions in these elements relative to UCC are most likely due to their high solubilities in natural waters. Their high solubilities prevent them from being precipitated with Fe–Mn oxyhydroxides and allow them to be easily leached from any detrital components remaining in the varnish.

Enrichments in rare-earth elements, Co, Ni and Pb: The high degree of enrichment in the REEs, Co, Ni and Pb is consistent with their particle-reactive nature [17]. These elements are roughly correlated with Mn enrichment, suggesting that they are either co-precipitated or scavenged by Mn oxyhydroxides.

Positive Ce anomalies: The anomalously high Ce/La ratios are best explained by differential adsorption of the REEs by Fe–Mn oxyhydroxides in the aqueous environment. In most magmatic processes, it is difficult to significantly fractionate Ce from La. However, under more oxidizing conditions, such as in most meteoric waters, a large fraction of Ce is in the +4 state, which differs from the dominant +3 valence state of the neighboring REEs. Ce thus has a higher ionic potential and is preferentially adsorbed onto colloid particles, such as Fe–Mn oxyhydroxides [18–20]. Ce anomalies are a common feature of waters and/or or authigenic phases in marine, riverine and soil environments.

Fractionated Y/Ho: In most magmatic processes, Y is considered to be a close analogue of the rare-earth element Ho. This is reflected in the typically constant Y/Ho ratios of most magmatic rocks. The Y/Ho ratio of the varnishes, however, is much lower than magmatic values, suggesting that an aqueous process may have been involved in their fractionations.

No enrichments in high field strength elements: The HFSEs (Nb, Ta, Zr, Hf) do not show significant enrichments contrary to the fact that these elements are very particle reactive once they are in solution. Their lack of enrichments thus suggests that this signature was inherited from an aqueous source initially depleted in the HFSEs. In general, these elements are much more insoluble than the REEs, Co, Ni and Pb and are therefore more difficult to leach from rocks or dust.

Fractionated Th/U: Given that fluid-absent magmatic processes cannot significantly fractionate Th from U, the more particle-reactive behavior of Th compared to U should lead us to predict that varnishes should have anomalously high Th/U ratios. On the contrary, depleted ratios are observed. We interpret the depleted Th/U ratios to be a feature that is largely inherited from a Th-poor aqueous source similar to the explanation given for the HFSEs (see above).

4.2. Testing models for varnish formation

Each of the models for varnish formation suggested above makes specific predictions on trace-element enrichments and fractionations (Fig. 4). These are summarized below.

Model 1: Varnishes form by direct leaching of the rock substrate followed by re-precipitation on the rock surface (Fig. 4A). This process predicts that

varnish grows from the inside to the outside, e.g., via accretion from within. This suggests that any trace metals leached from the rock substrate that are strongly adsorbed by Fe–Mn oxyhydroxides would be quantitatively (100%) sequestered in the varnish. Therefore, it would be difficult to significantly fractionate Ce from La. During dissolution of silicate rocks, Ce and La are not significantly fractionated. Because a large proportion of Ce is in the +4 state, Ce is preferentially scavenged by Fe–Mn oxyhydroxides relative to La. However, in the case where Ce and La are quantitatively removed, there can be no fractionation of Ce/La ratios.

Model 2: Varnishes form by slow (1000+ years) diagenesis of detrital dust particles *after* accretion to the rock substrate (Fig. 4B). In this scenario, the maximum enrichment in the concentration of a trace metal is equal to the inverse of the mass fraction remaining after diagenetic reactions have occurred. The loss of Si during clay formation is probably the dominant form of mass loss and yields a ~1.8-fold enrichment in trace elements that are either retained in the insoluble and/or clay residues or efficiently re-precipitated as Fe–Mn oxyhydroxides (this assumes that continental crust has ~70 wt.% SiO_2, clays have ~45 wt.% SiO_2 and aqueous Si is lost via SiO_2^0). Loss of other major elements, such as Al, Ca and Mg, can increase this enrichment factor of trace elements a little more. This scenario therefore predicts that insoluble elements, such as Th and the HFSEs, will be the most enriched.

Model 3: Varnishes form by direct chemical precipitation of dissolved atmospheric components in rain water, fog droplets or aerosols (Fig. 4C). In this scenario, the trace-element enrichments in varnish would be derived by scavenging and/or co-precipitation of aqueous trace metals in the atmosphere. The scavenging efficiency should be controlled to a certain extent by equilibrium partitioning and therefore the relative enrichments in trace metals should follow their partitioning behaviors. Strong fractionations, particularly, in Ce/La ratios are predicted.

It can be seen in Figs. 1–3 that the varnishes have trace-element abundance patterns significantly

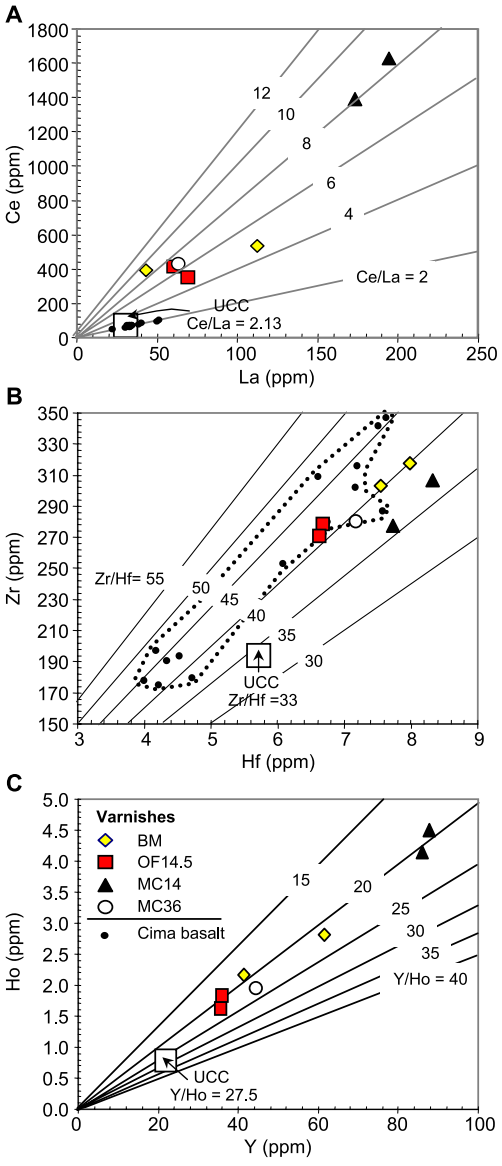

Fig. 2. (A) Ce (ppm) versus La (ppm). (B) Zr (ppm) versus Hf (ppm). (C) Ho (ppm) versus Y (Ho). Symbols as in Fig. 1. Duplicate symbols represent two separate dissolutions of unmixed powders scraped from the varnish surface. Solid lines represent contours of Ce/La (A), Zr/Hf (B) and Y/Ho (C) ratios. Small solid circles and dotted outlined region represent the Zr, Hf, Ce and La concentrations of Cima basalts. Upper continental crust (UCC) denoted by a large open square.

different from upper continental crust (UCC) and the underlying basaltic substrate. The most striking features are anomalously high Ce/La and low Th/U

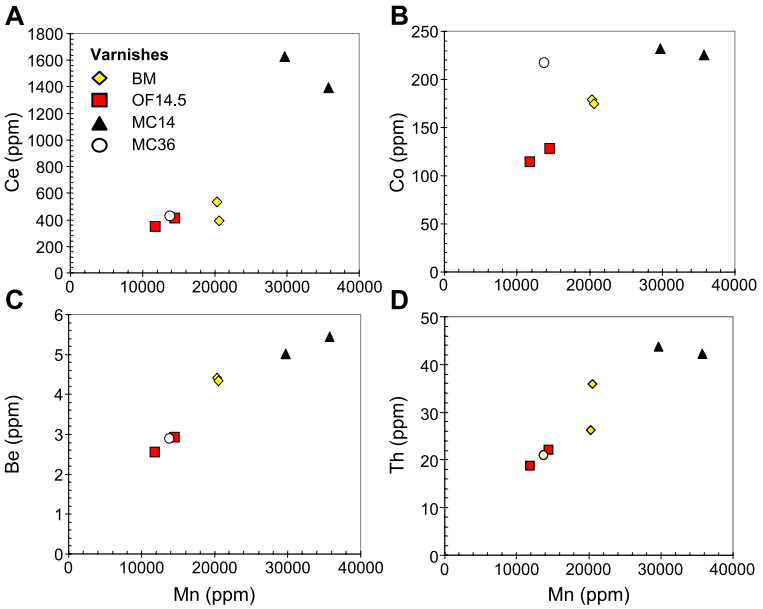

Fig. 3. Ce, Co, Ba and Be (ppm) versus Mn (ppm) in varnishes. Those samples with two symbols represent two different aliquots.

and Y/Ho ratios, which fall outside the range observed in magmatic processes. Due to the difficulty of fractionating Ce/La and Y/Ho during leaching, the fractionated ratios must be due to the effects of differential partitioning onto Fe–Mn oxyhydroxides. In light of our discussion of the models, this suggests that the trace-element enrichments do not originate from the rock substrate. The 2- to 40-fold enrichments of REEs and other metals (e.g., U, Ni, Co and Pb) and the 1–2 order-of-magnitude enrichments of Mn relative to UCC require >97% of the original mass to be lost, which far exceeds that predicted by diagenesis of dust particles alone. Such large enrichments can only be achieved if the residual dust or clay particles are physically removed after the varnish has formed. However, the preservation of coherent micro-laminations in varnish structures [2,21] indicates that post-depositional physical removal of clay or dust grains is unlikely. Moreover, the highly insoluble HFSEs are depleted relative to the more soluble elements (REEs, U, Ni, Co and Pb), which is opposite to that predicted by the diagenetic model.

We conclude that most of the trace-element enrichments and fractionations can be most easily explained if they derive from aqueous atmospheric components deposited on the rock substrate (Fig. 4C). We further suggest that leaching of dust particles in the atmosphere allows for the residual dust particles and aqueous components to be physically removed before or during deposition as varnish. Integrated over time, this allows for extreme trace-element enrichments and fractionations. We propose below a refined model for varnish formation.

4.3. A refined model for varnish formation: aqueous atmospheric deposition

We propose the following model for the origin of desert varnish. Small amounts of Fe^{2+} and Mn^{2+} cations are liberated by surface leaching/dissolution of airborne dust grains around which rain/fog droplets have nucleated. At the pH (5.7) and Eh conditions (~0.8) of rainwater, Mn is more soluble than Fe and so the dissolved Mn content is enhanced relative to the dissolved Fe content. Precipitation of Fe and Mn on rock substrates requires that these cations be oxidized to their insoluble trivalent states (possible oxidation mechanisms have been suggested by Dorn [4]). At the same time as Fe and Mn are leached from dust grains, labile trace metals, such as the REE, Co, Ni, Pb, Sr, Rb and Cs, are also released

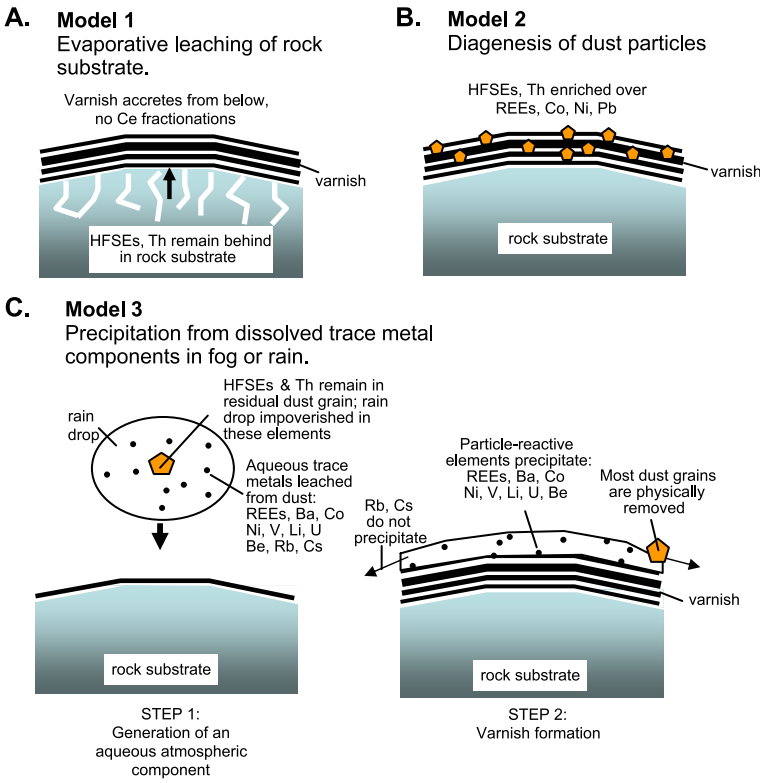

Fig. 4. Schematic diagrams of three scenarios for varnish formation: (A) Model 1: leaching of the rock substrate followed by precipitation at the rock surface, (B) Model 2: post-depositional diagenesis, wherein immobile element concentrations are enriched due to net mass loss of Al and Si during conversion of primary silicate minerals to clay minerals, (C) Model 2: direct aqueous atmospheric deposition wherein Fe, Mn and trace metals are leached from dust grains into rain/fog droplets, and residual dust/clay grains are physically separated from the aqueous component by water runoff or by wind.

into rain/fog droplets. Insoluble elements such as the HFSEs and Th largely remain behind in the dust grains so that these elements are highly depleted in the rain/fog droplets. When rain/fog droplets land on the rock surface, Fe–Mn oxyhydroxides and the particle-reactive trace metals present in the rain droplets are co-precipitated. The relative enrichment in trace metals must be controlled by equilibrium partitioning between rain/fog water and Fe–Mn oxyhydroxides [22] rather than by quantitative chemical precipitation as what might occur if the rain/fog droplets completely evaporated. This implies that there must have been an excess of rain/fog droplets, which ultimately flows off or is blown off (by wind) of the rock surface, leaving behind a small fraction of its trace metal content as varnish. Integrated over long periods of time, this can lead to extreme trace metal enrichments. Importantly, only a small fraction of the total amount of dust grains contributing to the dissolved trace metal budget will actually get deposited in the varnish. The majority of dust particles are physically removed before or during deposition by excess runoff of water or by wind. Highly soluble elements, such as Rb and Cs, are either never precipitated or removed during water runoff. The particle-reactive elements, once sequestered in the varnish, are not removed.

4.4. Similarities and differences with marine Fe–Mn crusts

Fe–Mn crusts formed in deep-sea marine environments may be a very remote analogue for varnish formation. It is generally believed that Fe–Mn

crusts form by direct precipitation of dissolved Fe, Mn and metals in seawater. They have elevated trace metal concentrations, positive Ce anomalies and depletions in Th relative to U (Fig. 1). It can be seen in Fig. 1 that Fe–Mn crusts are roughly enriched and depleted in the same elements. The enrichments in Pb, Co, Cr, REEs and, especially, Ce can all be explained by the tendency for these elements to adsorb onto Fe–Mn oxyhydroxide colloids. The lack of enrichments in HFSEs and Th can also be explained as a feature inherited from seawater, which is itself depleted in these largely insoluble elements. Rb and Cs, being highly soluble, are not precipitated with Fe–Mn oxyhydroxides, explaining the similarly depleted Rb and Cs contents of Fe–Mn crusts and varnishes. We recognize that the overall similarities in trace metal abundance patterns between Fe–Mn crusts and varnishes may be entirely fortuitous. However, we speculate that even though varnishes form in sub-aerial instead of marine environments, varnishes are essentially chemical precipitates from aqueous components in the atmosphere. In detail, however, some differences between the trace-element abundance patterns of varnish and Fe–Mn crusts (see Section 3.2) suggest that trace metal partitioning behaviors in subaerial and marine environments may be slightly different (as expected because the pH of seawater is ~ 8, which is higher than that of rainwater), and/or that the compositions of seawater and the atmospheric aqueous component are different. An important point to recognize is that there are many sinks that can modulate the trace-element composition of seawater, whereas in the case of the rain drops, the main sink may be Fe–Mn oxyhydroxides.

4.5. Implications

If our interpretations are correct, a direct aqueous atmospheric origin for varnish has important implications. Varnishes may be one of few substances that record pre-anthropogenic atmospheric levels of dissolved metals. If the partitioning of trace elements between varnish and rainwater can be quantified, it may be possible to use varnishes to estimate the proportion of atmospheric inputs into the ocean that is already in aqueous form or is immediately soluble. At the very least, microstratigraphic studies of varnish, when combined with trace-element work, can reveal how aqueous atmospheric components have varied through time. Because the solubility of trace metals in rainwater depends on pH, which itself depends on atmospheric CO_2 levels, variations in atmospheric CO_2 may result in subtle variations in the chemical make-up of varnishes. Finally, our observations that some varnishes have depleted Th/U ratios relative to UCC suggest that it may be worth re-investigating varnishes in the context of U–Th series dating. There is also the potential for further constraining the source of varnish through other radiogenic isotope systems. In this context, Nd and Pb isotopes may hold the most promise because both elements are strongly scavenged and hence retained for long periods of time by the Fe–Mn oxyhydroxide component. Finally, if Martian rock surfaces are also covered with Fe–Mn coatings exhibiting morphological and geochemical similarities to the terrestrial varnishes studied here, the possibility of an aqueous atmospheric origin on Mars should be investigated.

5. Conclusions

We investigated desert varnish in order to better understand their mode of formation. We found that these varnishes are highly enriched in many trace elements relative to upper continental crust. In particular, the relative patterns of enrichments require an aqueous origin that is best explained by direct aqueous atmospheric deposition. To explain our observations, we have proposed a refined model for varnish formation, where Fe, Mn and various trace metals are released into atmospheric rain/fog droplets, which have nucleated around dust aerosols. Upon contact with a smooth rock surface, Fe–Mn oxyhydroxides and particle-reactive trace metals are co-precipitated, and the residual aqueous fluid and dust particles are physically removed during water runoff or blown off by wind. The partitioning of particle-reactive trace metals between Fe–Mn oxyhydroxides and the aqueous phase can be considered to be an equilibrium process. Due to their nature of formation, varnishes may provide one of the only ways to estimate the trace-element composition of pre-anthropogenic rainwater.

Acknowledgements

Undergraduate research of Thiagarajan was made possible by support from the Department of Earth Science at Rice University and, in part, by an NSF grant to Lee (EAR-0309121). The comments of anonymous reviewers are greatly appreciated. ***[BOYLE]***

References

[1] W.S. Broecker, T. Liu, Rock varnish: recorder of desert wetness? Geol. Soc. Am. Today 11 (2001) 4–10.
[2] R.M. Potter, G.R. Rossman, Desert varnish: the importance of clay minerals, Science 196 (1977) 1446–1448.
[3] D. Kringsley, Models of rock varnish formation constrained by high resolution transmission electron microscopy, Sedimentology 45 (1998) 711–725.
[4] R.I. Dorn, Rock Coatings, Elsevier, Amsterdam, 1998, 429 pp.
[5] R.I. Dorn, T.M. Oberlander, Microbial origin of desert varnish, Science 213 (1981) 1245–1247.
[6] H. Bao, G.M. Michalski, M.H. Thiemens, Sulfate oxygen-17 anomalies in desert varnishes, Geochim. Cosmochim. Acta 65 (2001) 2029–2036.
[7] M. Fleisher, T. Liu, W.S. Broecker, W. Moore, A clue regarding the origin of rock varnish, Geophys. Res. Lett. 26 (1999) 103–106.
[8] T. Liu, Blind testing of rock varnish microstratigraphy as a chronometric indicator: results on late Quaternary lava flows in the Mojave Desert, Geomorphology 53 (2003) 209–234.
[9] B. Nagy, L.A. Nagy, M.J. Rigali, W.D. Jones, D.H. Krinsley, N. Sinclair, Rock varnish in the Sonoran desert: microbiologically mediated accumulations of manganiferous sediments, Sedimentology 38 (1991) 1153–1171.
[10] E.J. Israel, R.E. Arvidson, A. Wang, J.D. Pasteris, B.L. Jolliff, Laser Raman spectroscopy of varnished basalt and implications for in situ measurements of Martian rocks, J. Geophys. Res. 102 (1997) 28705–28716.
[11] R.L. Mancinelli, J.L. Bishop, Mangetite in desert varnish and applications to rock varnish on Mars, Lunar Planet. Sci. 33 (2002) 1046.
[12] B.D. Turrin, J.C. Dohrenwend, R.E. Drake, G.H. Curtis, K–Ar ages from the Cima volcanic field, eastern Mojave Desert, California, Isochron/West 44 (1985) 9–16.
[13] S.G. Wells, J.C. Dohrenwend, L.D. McFadden, B.D. Turrin, K.D. Mahrer, Late Cenozoic landscape evolution on lava flow surfaces of the Cima volcanic field, Mojave Desert, California, Geol. Soc. Amer. Bull. 96 (1985) 1518–1529.
[14] A.J. Bauman, Desert varnish and marine ferromanganese oxide nodules: congeneric phenomena, Nature 259 (1976) 387–388.
[15] R.L. Rudnick, D.M. Fountain, Nature and composition of the continental crust: a lower crustal perspective, Rev. Geophys. 33 (1995) 267–309.
[16] G.L. Farmer, A.F. Glazner, H.G. Wilshire, J.L. Wooden, W.J. Pickthorn, M. Katz, Origin of late Cenozoic basalts at the Cima volcanic field, Mojave Desert, California, J. Geophys. Res. 100 (1995) 8399–8415.
[17] M.A. Saito, J.W. Moffett, Temporal and spatial variability of cobalt in the Atlantic Ocean, Geochim. Cosmochim. Acta 66 (2002) 1943–1953.
[18] Y.-G. Liu, M.R.U. Miah, R.A. Schmitt, Cerium: a chemical tracer for paleo-oceanic redox conditions, Geochim. Cosmochim. Acta 52 (1988) 1361–1371.
[19] D.J. Piepgras, S.B. Jacobsen, The behavior of rare earth elements in seawater: precise determination of variations in the North Pacific water column, Geochim. Cosmochim. Acta 56 (1992) 1851–1862.
[20] D.S. Alibo, Y. Nozaki, Rare earth elements in seawater: particle association, shale-normalization, and Ce oxidation, Geochim. Cosmochim. Acta 63 (1999) 363–372.
[21] R.S. Perry, J.B. Adams, Desert varnish: evidence for cyclic deposition of manganese, Nature 276 (1978) 489–491.
[22] C.-K.D. Hsi, D. Langmuir, Adsorption of uranyl onto ferric oxyhydroxides: application of the surface complexation site-binding model, Geochim. Cosmochim. Acta 49 (1985) 1931–1941.